Research Square

Preprints are preliminary reports that have not undergone peer review.
They should not be considered conclusive, used to inform clinical practice,
or referenced by the media as validated information.

# Combined application of PRP gel and low-intensity pulsed ultrasound enhances early tendon-to-bone interface healing after acute rotator cuff repair in rats

**Junhong Chen**
Suining Central Hospital
**Qingshan Li**
Suining Central Hospital
**Libin Li**
Suining Central Hospital
**Xin Guo**
Suining Central Hospital
**Zhiqiang Wang**
Suining Central Hospital
**Xu Peng**
20259086@cdutcm.edu.cn
Chongqing Medical University
**Qiuling Shi2**
Chongqing Medical University

**Article**

**Keywords:**

**Posted Date:** November 6th, 2026

**DOI:** https://doi.org/10.21203/rs.3.rs-11400673/v1

**License:** This work is licensed under a Creative Commons Attribution 4.0 International License.
Read Full License

**Additional Declarations:** No competing interests reported.

# Combined application of PRP gel and low-intensity pulsed ultrasound enhances early tendon-to-bone interface healing after acute rotator cuff repair in rats

Junhong Chen[1], Qingshan Li[3], Libin Li[3], Xin Guo[3], Zhiqiang Wang[3], Xu Peng[2,3*] and Qiuling Shi[2*]

**Abstract**

**Objective** This study evaluated the effects of combined platelet-rich plasma (PRP) gel and low-intensity pulsed ultrasound (LIPUS) on early tendon – bone interface healing after acute rotator cuff repair in rats, using histological, micro-CT and biomechanical assessments to inform postoperative rehabilitation.

**Methods** Ninety SPF-grade male Sprague-Dawley rats (8 – 9 weeks old, 300 – 350 g) were used: 80 underwent left-sided rotator cuff injury and repair and were randomly allocated into four groups (n = 20 each: CON, LIPUS, PRP, P+L), and the remaining 10 served as blood donors for PRP preparation. Within each group, 10 animals were euthanized at postoperative week 4 and 10 at week 8. At each time point, 5 animals per group were processed for micro-CT and histological analysis and the other 5 for biomechanical testing.

**Results** At both time points, the combined group showed significantly higher bone volume fraction, trabecular thickness and number, fibrocartilage layer thickness, collagen fibre organization, ultimate load and stiffness than the other three groups ($P < 0.05$). LIPUS and PRP alone also improved these parameters over controls, but the combined regimen produced the most pronounced enhancement.

**Conclusion** Collectively, the combined application of PRP gel and LIPUS further promotes early tendon-to-bone healing after acute rotator cuff repair, substantially improving local tissue structure and biomechanical properties.

*Correspondence:

Xu Peng

20259086@cdutcm.edu.cn

Qiuling Shi

qshi@cqmu.edu.cn

**Background：**

Rotator cuff tears are pathological or structural disruptions of the rotator cuff muscles, arising from degenerative changes or traumatic forces. The condition accounts for 17–41% of all shoulder joint disorders[1]. Surgical repair remains the primary clinical intervention for medium-to-large rotator cuff tears; however, suboptimal healing at the tendon–bone interface (TBI) and persistently high retear rates constitute major unresolved clinical challenges[2]. The TBI is a structurally complex gradient zone composed sequentially of tendon, unmineralized fibrocartilage, mineralized fibrocartilage and bone[3]. This highly ordered hierarchical architecture plays a critical role in modulating load transmission and mitigating local stress concentrations at the bone and tendon/ligament junctions[4]. The healing process at this interface is protracted and intricate, rendering effective postoperative functional restoration a significant clinical hurdle in sports medicine[5].

Platelet-rich plasma (PRP) is an autologous concentrate of growth factors and cytokines, and its potential to promote tissue healing after rotator cuff repair has been extensively investigated[6, 7]. Nevertheless, liquid PRP is prone to rapid dispersion and uncontrolled release kinetics in vivo, which has led to considerable controversy regarding its clinical efficacy[8-10]. To address these limitations, PRP gel formulations activated by thrombin and calcium gluconate have been developed. Such gels form a fibrin scaffold that serves as a sustained-release depot for growth factors, thereby improving local retention, enhancing the regenerative microenvironment and prolonging the duration of bioactivity[11].

Low-intensity pulsed ultrasound (LIPUS) is a non-invasive physical therapy that transmits low-energy pulsed mechanical stimuli into target tissues. Through acoustic radiation force, micro-shear stress at the cell membrane and subsequent activation of mechanosensitive ion channels and integrin-associated signalling, LIPUS modulates cellular metabolism and downstream molecular pathways, thereby facilitating tissue

repair and regeneration[12]. This technology has been widely applied in orthopaedics, sports medicine, wound healing and neurological rehabilitation, offering advantages such as non-invasiveness, high safety and ease of operation[13].

Although PRP and mechanical stimulation have each shown promise in tendon-bone repair, evidence for combining them is only beginning to emerge. Peng et al. reported that PRP combined with mechanical stimulation enhanced early rotator-cuff healing in mice, with a larger fibrocartilage area, improved subchondral bone architecture and higher failure loads[14]. The mechanical stimulus in that study was delivered through active treadmill exercise, which depends on animal participation and cannot be readily applied, or tightly dosed, during the early postoperative period when the repaired construct is most vulnerable. Whether PRP can be combined with a non-invasive, locally delivered and precisely dose-controlled mechanical stimulus that is safe to start immediately after surgery remains unexamined. Low-intensity pulsed ultrasound (LIPUS) provides such a stimulus by transmitting low-energy acoustic radiation force and membrane micro-shear stress without requiring active movement. In addition, whether a thrombin/calcium-activated PRP gel, which forms a sustained-release fibrin scaffold rather than rapidly dispersed liquid PRP, can be paired with LIPUS has not been tested. We therefore hypothesized that combining PRP gel with LIPUS enhances early tendon-to-bone healing after acute rotator cuff repair through additive or synergistic, complementary mechanisms that improve both structural reconstruction and mechanical properties

## 1.Materials and Methods

### 1.1 Materials

#### 1.1.1 Animals

This animal experiment was approved by the Animal Ethics Committee of Suining Central Hospital (approval No. SYDWLL21-2411-6). All methods were performed in accordance with the relevant guidelines and regulations, and the study is reported in accordance with the ARRIVE 2.0 guidelines. All animal procedures were carried out in compliance with the institutional and national regulations for the humane care and use of laboratory animals, including the Chinese Regulations for the Administration of

Affairs Concerning Experimental Animals and the Guiding Opinions on the Treatment of Laboratory Animals, and the study was conducted in accordance with the 3R principles (replacement, reduction and refinement). A total of 90 healthy male specific-pathogen-free (SPF) Sprague–Dawley rats, aged 8–9 weeks and weighing 300–350 g, were obtained from Beijing HFK Bioscience Co., Ltd. (licence No. SCXK (Beijing) 2019-0008). All animals were housed under a 12-h light/dark cycle. Of these, 80 were used for the rotator cuff injury and repair model. The remaining 10 served as blood donors, from which PRP was prepared in batches throughout the study under anesthesia; donor rats were euthanized by an overdose of the same anesthetic after each terminal blood collection. The animals were group-housed at four per cage, fed a standard diet and given free access to food and water. Cages were regularly cleaned and disinfected, and adequate space was provided for activity to ensure animal welfare.

1.1.2 Reagents and materials

The low-intensity pulsed ultrasound (LIPUS) device was obtained from Chongqing Ronghai Medical Technology Co., Ltd. (Chongqing, China). EDTA decalcification solution, haematoxylin and eosin (H&E) staining solution, safranin O–fast green staining solution, and Masson's trichrome staining solution were purchased from Wuhan Servicebio Technology Co., Ltd. (Wuhan, China). 2.5% tribromoethanol was sourced from Shanghai Aladdin Biochemical Technology Co., Ltd. (Shanghai, China). Sodium citrate anticoagulant and calcium chloride were acquired from Beyotime Biotechnology (Shanghai, China). Lyophilized thrombin powder was obtained from Hunan Yige Pharmaceutical Co., Ltd. (Hunan, China), and calcium gluconate injection from Sichuan Meidakanghua Pharmaceutical Co., Ltd. (Sichuan, China). 4-0 polydioxanone (PDS) sutures were supplied by Johnson & Johnson (USA).

1.2 Method

1.2.1 PRP gel preparation

PRP was prepared in batches from the 10 donor rats. For each batch, one donor rat was anaesthetized by intraperitoneal injection of 2.5% tribromoethanol (1 mL per 100 g body weight), secured on a board, and the abdominal area was shaved and

disinfected. A 10-mL syringe pre-filled with 1 mL of sodium citrate anticoagulant was used to puncture the heart at the point of maximal pulsation, and 8 – 10 mL of arterial blood was withdrawn, gently agitated and transferred to anticoagulant tubes. The donor rat was then euthanized by an overdose of the same anesthetic. Blood from each batch was processed immediately through the two-step centrifugation protocol described below, and the resulting PRP gel was used for surgeries scheduled within the same batch. PRP was prepared by a two-step centrifugation method following Landesberg[15]. Briefly, whole blood was first centrifuged at 200g for 15 min at 20 ° C. After separation (platelet-poor plasma in the upper layer, buffy coat in the middle, and erythrocytes at the bottom), the middle and upper fractions were aspirated, pooled, and centrifuged again at 300g for 10 min. Most of the supernatant was discarded, and approximately one-tenth of the volume of the pellet was retained and resuspended to obtain PRP. A small aliquot was taken for platelet counting; only preparations with a platelet concentration at least three times that of whole blood were deemed acceptable. An activator solution (1000 U/mL thrombin in 10% calcium gluconate) was prepared, and PRP was mixed with the activator at a 10:1 volume ratio and allowed to stand until gelation occurred.

1.2.2 Surgical model of rotator cuff injury

The rotator cuff injury and repair model was established according to the protocol of Deng et al[16]. Rats were anaesthetized with an intraperitoneal injection of 2.5% tribromoethanol (1 mL/100 g) and placed in right lateral recumbency. The left shoulder was shaved with a depilatory cream (10 min application) and the skin disinfected with iodophor. The left forelimb was fixed in adduction and external rotation to expose the surface landmarks of the humeral head. A longitudinal incision was made, and blunt dissection through the subcutaneous tissue exposed the deltoid muscle. Using the L-shaped vessel on the deltoid surface as an anatomical landmark, the acromioclavicular joint was exposed and gently elevated. The deltoid was partially dissected to reveal the rotator cuff, followed by blunt dissection of its deep layer to expose the supraspinatus tendon. A 4-0 polydioxanone (PDS) suture was placed in a figure-of-eight pattern for tendon traction, and the tendon was transected flush with its

humeral insertion. Residual fibrocartilage at the insertion site was debrided. Two oblique bone tunnels crossing in a figure-of-eight configuration were drilled on both sides of the insertion using a 5-mL syringe needle (anterior tunnel directed posteroinferiorly, posterior tunnel directed anteroinferiorly). The pre-placed suture was passed through the tunnels, tightened and tied. After confirming the stability of the reconstruction, the incision was closed in layers, re-disinfected and covered with sterile gauze.

1.2.3 Experimental groups

Eighty male Sprague-Dawley rats (8–9 weeks old, 300–350 g) underwent left-sided rotator cuff injury and repair and were randomly assigned to four groups (n = 20 each: CON, LIPUS, PRP, P+L). Within each group, animals were randomized 1:1 to a week-4 or a week-8 euthanasia cohort (n = 10 per time point per group). At each time point, 5 animals per group were further randomized for micro-CT followed by histological analysis, and the other 5 for biomechanical testing, so that each endpoint used different animals and no animal underwent repeated sampling. Immediately after repair, the injury site was filled with an equal volume of saline in the CON and LIPUS groups, whereas 0.2 mL of PRP gel was applied at the supraspinatus tendon–humeral interface in the PRP and P+L groups. From postoperative week 1, the CON and PRP groups received sham LIPUS, while the LIPUS and P+L groups received active LIPUS (power density 30 mW/cm$^2$, frequency 1.5 MHz, repetition frequency 1 kHz, duty cycle 20%)[17] for five sessions per week. At 4 and 8 weeks after surgery, mice were euthanized (0.3% pentobarbital sodium, 1.5 mL/20 g, by an intraperito-neal injection), and the SST–humeral complex (SSTH) was harvested.

1.2.4 Histological staining

Histological analysis was performed on 5 animals per group per time point, using the same specimens that had undergone micro-CT. Fresh supraspinatus tendon–humeral (SSTH) specimens were fixed in 4% paraformaldehyde for 24 h and then decalcified in 10% ethylene diamine tetraacetic acid (EDTA) solution for 14 days. After dehydration through a graded ethanol series and paraffin embedding, the tissues were

sectioned coronally at 5 μm thickness through the supraspinatus tendon and the greater tuberosity region. Serial sections were stained with haematoxylin and eosin (H&E), Masson's trichrome, and safranin O/fast green, all of which were purchased from Wuhan Servicebio Technology Co., Ltd. (Wuhan, China). H&E staining was used for general histological assessment of the tendon–bone interface; safranin O/fast green staining evaluated fibrocartilage repair; and Masson's trichrome staining visualized collagen fibre arrangement and interface maturity. All sections were examined under identical conditions using a transmitted-light microscope (Olympus CX31, Olympus Inc., Hamburg, Germany).

1.2.5 Micro-CT analysis

Trabecular bone architecture around the tendon attachment site was evaluated using micro-computed tomography (Micro-CT, Skyscan1276, Bruker, Germany). Micro-CT was performed on 5 animals per group per time point; after scanning, the same fixed specimens were decalcified and processed for the histological analysis described above. Specimens intended for Micro-CT were first fixed in 4% paraformaldehyde at 4 °C for 24 h, then transferred to tubes containing 0.9% saline and stored at room temperature until scanning. Scans were performed at a tube current of 200 μA, a tube voltage of 70 kV, an isotropic voxel size of 6.534165 μm, an exposure time of 350 ms, and a rotation angle of 180°. Raw data were reconstructed using NRecon software (version V1.7.4.2, Bruker, Germany) with a region-of-interest (ROI) approach. Reconstruction settings included a smoothing factor of 5, beam-hardening correction of 8, and ring-artifact correction of 25%. After initiating the reconstruction pipeline on the selected data folders, the resulting images were analysed with CT Analyser (version 1.20.3.0, Bruker, Germany). The following parameters were measured at the tendon–bone interface: bone volume fraction (BV/TV), trabecular thickness (Tb.Th), trabecular number (Tb.N) and trabecular separation (Tb.Sp).

1.2.6 Biomechanical testing

>Biomechanical testing was performed on a separate set of 5 animals per group per time point. The soft tissues surrounding each SSTH complex were carefully dissected,

and the complexes were stored at −80 °C until use. Before testing, the SSTH complexes were thawed at room temperature and maintained in a 0.9% saline bath at 37 °C. The supraspinatus muscle, surrounding soft tissues and all sutures were carefully removed. The humerus was secured in a testing fixture, and the supraspinatus tendon was attached to a custom-made clamp using sandpaper and ethyl cyanoacrylate adhesive. The specimens were mounted in a microcomputer-controlled electronic material testing system (Shanghai Hengyi Instrument Equipment Co., Ltd., Shanghai, China) at an abduction angle of approximately 60°. After three preconditioning cycles under a preload of 0–0.5 N, tensile loading was applied to the tendon at a rate of 3 mm/s until failure. The failure load was recorded, and stiffness was calculated from the linear region of the load–deformation curve.

1.3 Statistical analysis

All quantitative data are expressed as mean ± standard deviation (SD). For in vivo assessments, animals were euthanized at two prespecified time points, 4 and 8 weeks postoperatively. At each time point, differences among the four groups were compared using one-way analysis of variance (ANOVA) followed by Bonferroni post hoc correction, with n = 5 per group for each endpoint (the micro-CT/histology and biomechanical cohorts were analysed separately). Because different animals were euthanized at each time point, within-group changes over time were not formally assessed. Normality was assessed by the Shapiro–Wilk test; non-normally distributed outcomes were analysed by the Kruskal–Wallis test with Dunn's post-hoc correction. Statistical analyses were performed using SPSS 27.0 (IBM, Armonk, NY, USA) and GraphPad Prism 10.0 (GraphPad Software, San Diego, CA, USA). A two-sided P value $< 0.05$ was considered statistically significant.

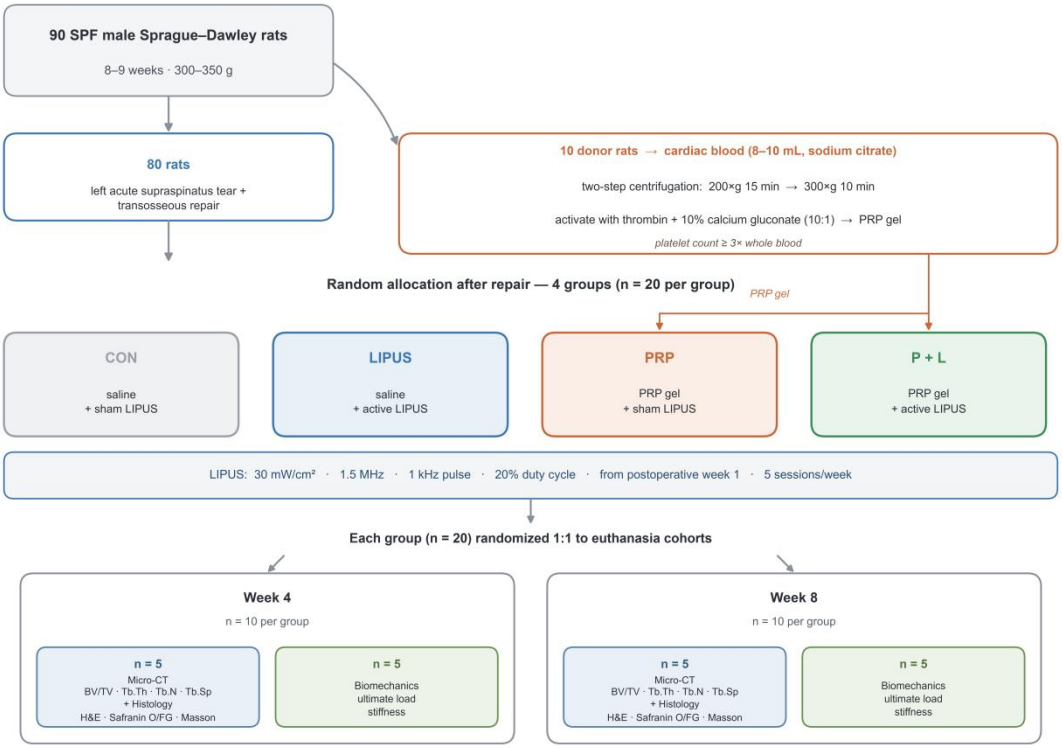



Figure 1 | Experimental design and workflow. Ninety male Sprague–Dawley rats were used: 80 underwent acute supraspinatus tear and transosseous repair and were randomized into four groups (CON, LIPUS, PRP, P+L; n = 20 per group), and 10 served as blood donors for PRP-gel preparation. Each group was randomized 1:1 to week-4 or week-8 euthanasia (n = 10 per time point); at each time point, 5 animals were analysed by micro-CT and histology and 5 by biomechanical testing.

## 2 Results

### 2.1 HE staining

At 4 weeks post-surgery, histological examination revealed marked scar tissue hyperplasia at the tendon–bone interface in all groups, with disruption of the normal four-layer gradient architecture characteristic of the native enthesis. Cellular arrangement within the interface region lost its regular orientation, and tissue interconnectivity was diminished. Although all experimental groups exhibited some degree of healing, intergroup differences were evident in the progression and histological features. Among them, the P+L group demonstrated the best tissue continuity, with relatively well-ordered cellular and collagen fibre alignment,

surpassing the other three groups. The LIPUS group showed more regular cellular and fibre arrangement than the PRP and CON groups, whereas the CON group displayed the poorest healing outcome. At 8 weeks post-surgery, tissue continuity and structural organization improved across all groups as healing advanced. The P+L group continued to exhibit the most favourable healing, characterized by orderly cellular and fibre arrangement, a discernible tidemark, and evidence of fibrocartilage layer reconstruction. Both the LIPUS and PRP groups showed marked advantages over the CON group in terms of tendon fibre density and tissue architecture. Representative H&E-stained sections of the tendon – bone interface from all four groups at both time points are shown in Fig. 2.

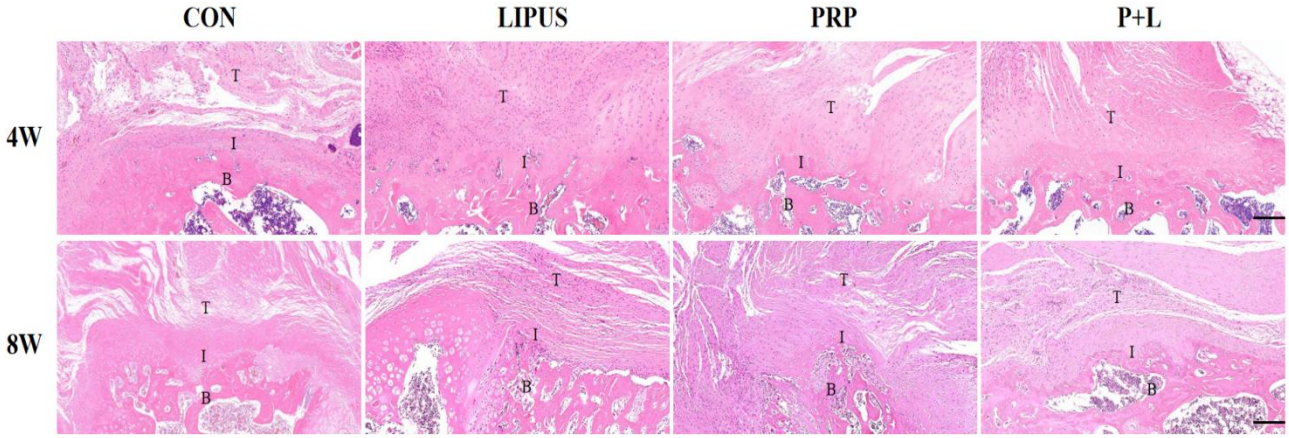



Figure 2 | Representative H&E-stained sections of the tendon – bone interface from all four groups at 4 and 8 weeks post-surgery. Although healing was evident in each experimental group, intergroup variations were observed in both the progression and histological features. The combined (P+L) group exhibited the greatest tissue continuity, with relatively well-ordered cellular and collagen fibre alignment, and demonstrated superior healing outcomes compared with the other three groups. Scale bar, 100 μ m.

## 2.2 Safranin O/fast green staining

At 4 weeks post-surgery, histological examination revealed distinct fibrocartilaginous tissue formation accompanied by endochondral ossification at the tendon – bone interface in the P+L group, with histological features that differed markedly from those of the other three groups. The thickness of the newly formed fibrocartilage layer was significantly greater in the P+L group than in the LIPUS and PRP groups ($P <$

0.05), whereas no discernible fibrocartilage layer was observed in the CON group at this time point. By 8 weeks, all groups exhibited varying degrees of structural repair at the interface. Compared with the 4-week time point, the overall quality of tendon–bone healing had improved in all groups, and fibrocartilage formation was histologically detectable in each. Notably, a relatively typical four-layer gradient architecture was observed in both the P+L and LIPUS groups, with significantly more chondrocytes and well-demarcated cartilage zones compared with the other groups. Among them, the P+L group displayed the most pronounced regenerative effect, with an intact and distinctly layered interface, substantially outperforming the other three groups. In contrast, the CON group showed only a thin fibrocartilage layer, indicating comparatively limited interface restoration. Representative safranin O/fast green-stained sections are shown in Fig. 3.

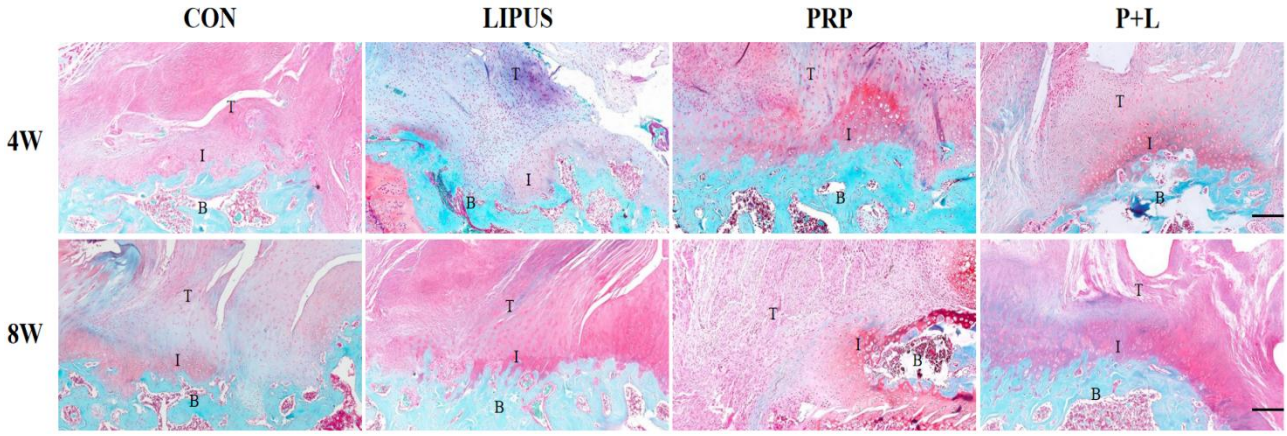



Figure 3 | Representative safranin O/fast green-stained sections of the tendon–bone interface from all groups at 4 and 8 weeks post-surgery. Varying degrees of structural repair were observed across groups. The P+L group exhibited a greater thickness of the newly formed fibrocartilage layer compared with the LIPUS and PRP groups. Scale bar, 100 μm.

## 2.3 Masson's trichrome staining

At 4 weeks post-surgery, the collagen fibres at the tendon–bone interface in the P+L group appeared more densely packed, with superior continuity and parallel alignment compared with the other experimental groups. In contrast, the LIPUS and PRP groups exhibited relatively disorganized collagen arrangement and poorer interface structural regularity, whereas the CON group displayed a disordered fibre orientation lacking

functional directionality. By 8 weeks, all groups showed varying degrees of structural restoration. The P+L group presented abundant, densely distributed collagen fibres with regular organization, well-aligned chondrocytes, and evidence of vascular ingrowth. The LIPUS group showed relatively compact collagen fibre connections with good continuity, while the CON group, despite an increased fibre content, still demonstrated a suboptimal fibre arrangement. Collectively, these Masson staining observations indicate that the P+L group was superior to the other three groups in both collagen fibre quantity and organizational regularity, suggesting the most favourable tendon–bone healing quality. Representative Masson's trichrome-stained sections are shown in Fig. 4.

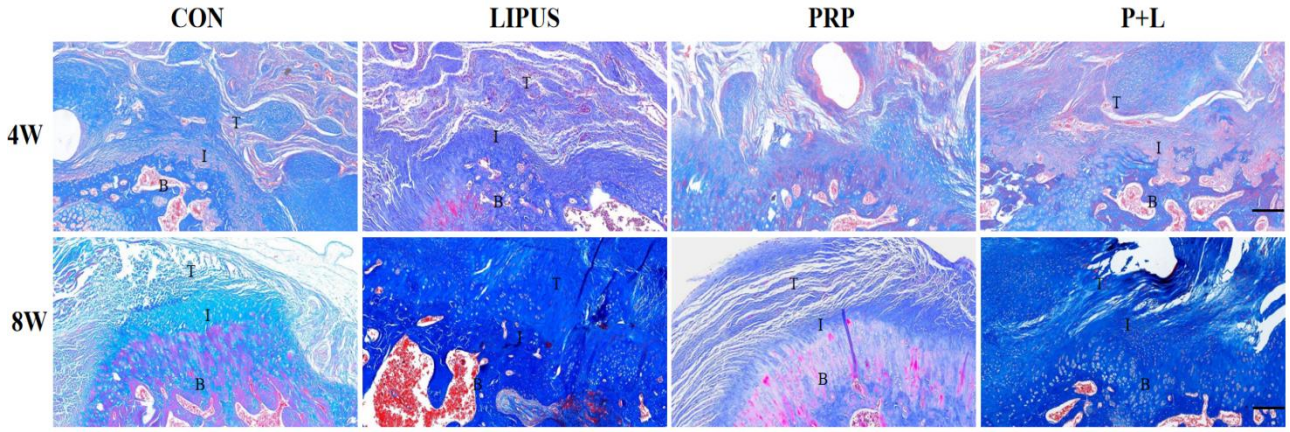



Figure 4 | Representative Masson's trichrome-stained sections of the tendon–bone interface from all groups at 4 and 8 weeks post-surgery. Varying degrees of structural repair were observed across groups. The P+L group displayed abundant, densely distributed collagen fibres with regular alignment, well-ordered chondrocytes, and vascular ingrowth at the interface. Scale bar, 100 μm.

## 2.4 Micro-CT analysis

To evaluate the effects of combined PRP and LIPUS application on subchondral bone quality at the tendon–bone interface, Micro-CT imaging and three-dimensional reconstruction were performed on the harvested specimens, with subsequent quantitative analysis of the region of interest (ROI). At 4 weeks post-surgery, the P+L group exhibited significantly higher values of BV/TV, Tb.Th and Tb.N compared with the LIPUS, PRP and CON groups (all $P < 0.05$), and a significantly lower Tb.Sp than the other three groups ($P < 0.05$). The LIPUS group showed a significantly higher

BV/TV than the CON group ($P < 0.05$), and the PRP group also demonstrated significantly higher BV/TV and Tb.Th than the CON group ($P < 0.05$). However, no significant differences were observed between the LIPUS and PRP groups in any of the bone morphometric parameters, including BV/TV, Tb.Th, Tb.N and Tb.Sp (all $P > 0.05$). At 8 weeks post-surgery, BV/TV and Tb.Th remained significantly higher in the P+L group than in the LIPUS, PRP and CON groups ($P < 0.05$), whereas Tb.Sp was significantly lower in the P+L group than in all other groups ($P < 0.05$). The LIPUS group showed significantly higher BV/TV, Tb.Th and Tb.N than the CON group ($P < 0.05$), and the PRP group also exhibited significantly higher BV/TV and Tb.N than the CON group ($P < 0.05$). Both the LIPUS and PRP groups had significantly lower Tb.Sp than the CON group ($P < 0.05$). However, no statistically significant differences were found between the PRP and LIPUS groups in any of the bone morphometric parameters ($P > 0.05$).Quantitative comparisons of bone morphometric parameters among the four groups are summarized in Fig. 5 and Fig. 6.

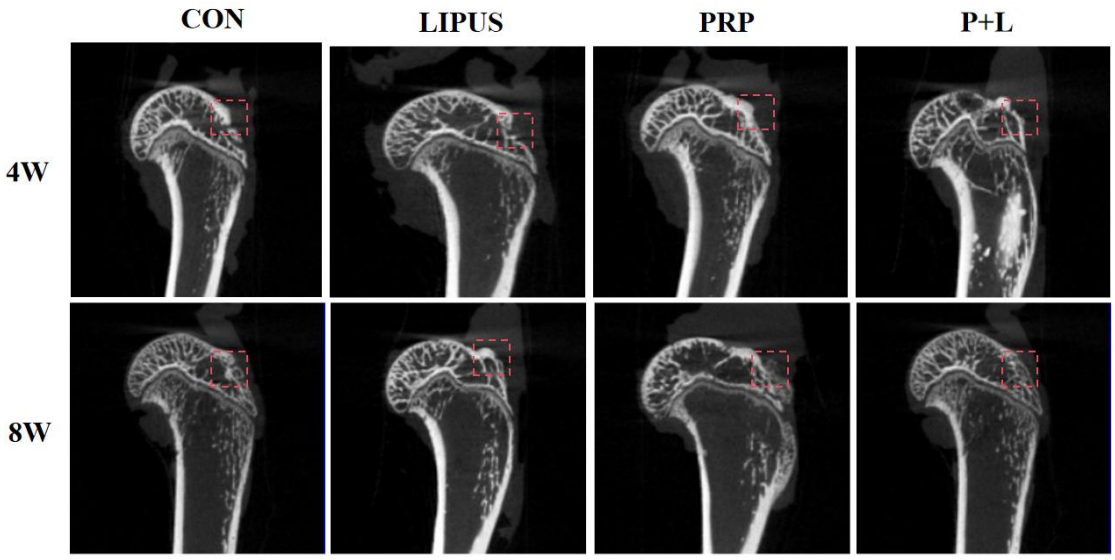



Figure 5. Micro-computed tomography (micro-CT) of the supraspinatus tendon – humeral complex at 4 and 8 weeks after surgery. Sagittal sections are shown for each time point. Dashed boxes delineate the selected regions of interest (ROIs)



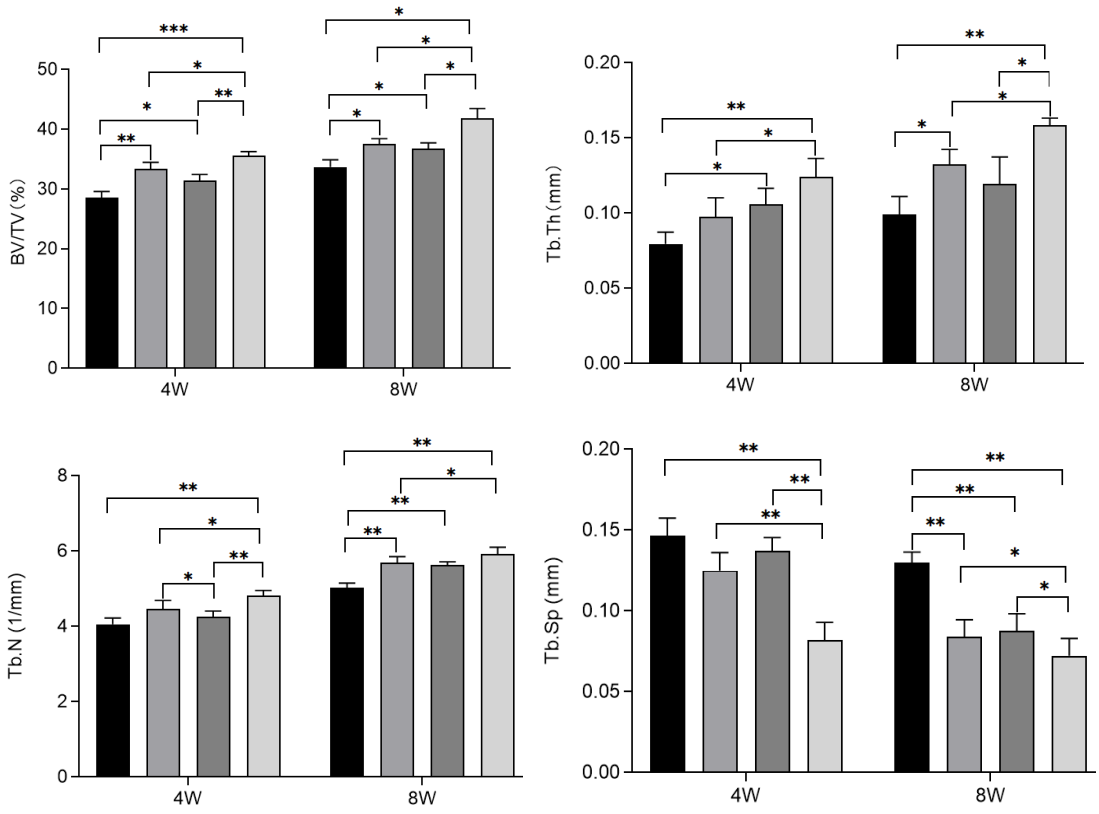



Figure 6 | Comparison of bone morphometric parameters among the control (CON), LIPUS, PRP and combined (P+L) groups at 4 and 8 weeks post-surgery. The P+L group exhibited significantly higher BV/TV, Tb.Th and Tb.N, and significantly lower Tb.Sp, compared with the other three groups at both time points. BV/TV, bone volume fraction; Tb.Th, trabecular thickness; Tb.N, trabecular number; Tb.Sp, trabecular separation. $P < 0.05$.

## 2.5 Biomechanical testing

The ultimate load and stiffness in all groups increased with healing time. At both 4 and 8 weeks post-surgery, the P+L group demonstrated significantly higher ultimate load and stiffness than the other three groups ($P < 0.05$). At each time point, the LIPUS-alone group also showed significantly greater ultimate load and stiffness compared with the control group ($P < 0.05$). At 4 weeks, no significant differences in ultimate load or stiffness were observed between the PRP and LIPUS groups ($P > 0.05$); however, at 8 weeks, stiffness was significantly higher in the LIPUS group than in the PRP group ($P < 0.05$). Collectively, these results indicate that combined PRP and LIPUS treatment further enhances the repair of the tendon‑bone interface, producing the greatest improvement in biomechanical properties. Ultimate load and

stiffness of the tendon－bone interface are summarized in Fig. 7.

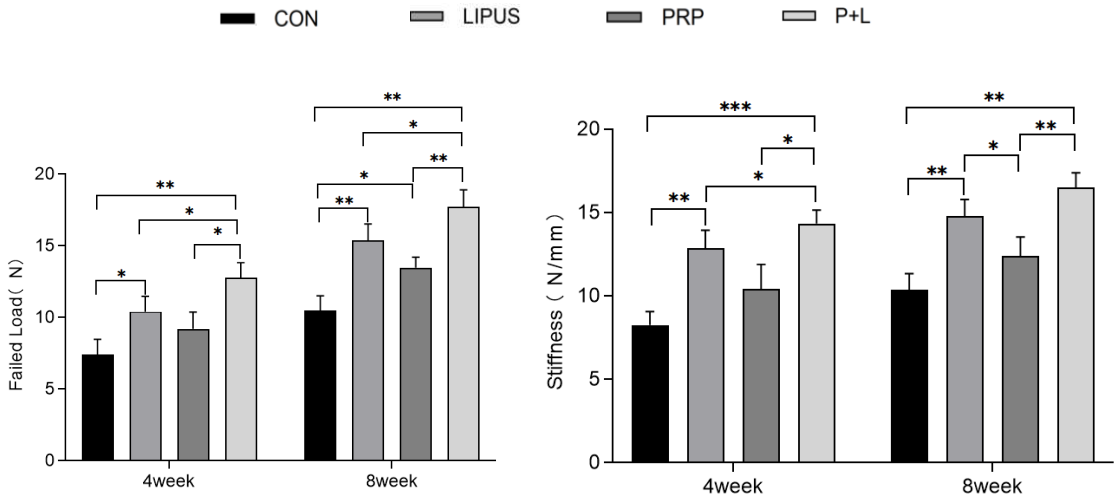



Figure 7 | Biomechanical properties of the tendon－bone interface in the CON, LIPUS, PRP and P+L groups at 4 and 8 weeks post-surgery. At both time points, the P+L group exhibited significantly higher ultimate load and stiffness than the other three groups ($P < 0.05$). Ultimate load and stiffness are expressed as mean ± SD. $P < 0.05$.

## Discussion

Rotator cuff injury is one of the most common shoulder disorders in clinical practice, and arthroscopic rotator cuff repair has become the gold-standard surgical procedure for treating rotator cuff tears[18]. However, the persistently high retear rate resulting from suboptimal tendon－bone interface healing remains a major challenge for sports medicine practitioners[19]. The native enthesis is a gradient transitional zone composed of tendon, fibrocartilage, calcified cartilage and bone, and is essential for effective load transmission and stress distribution[20].

Following surgical repair, however, the tendon－bone interface typically heals via scar tissue with poor mechanical properties, failing to restore the original gradient architecture—a fundamental cause of repair failure. Hence, there is considerable clinical interest in identifying adjuvant therapies that can effectively promote high-quality healing at the tendon－bone interface. In the present study, using a rat model of acute rotator cuff injury, we systematically compared the effects of PRP gel, LIPUS and their combination on early tendon－bone interface healing. The combined

treatment yielded the most favourable outcomes across histological, radiological and biomechanical assessments. The main findings and their clinical implications are discussed below. In this study, the PRP gel group exhibited significantly greater bone volume fraction, fibrocartilage layer thickness and biomechanical properties than the control group at both 4 and 8 weeks post-surgery, consistent with previous reports. The biological basis for PRP-mediated enhancement of tendon–bone healing lies in the abundant growth factors released upon platelet activation, including platelet-derived growth factor (PDGF), transforming growth factor-β (TGF-β), vascular endothelial growth factor (VEGF) and basic fibroblast growth factor (bFGF)[21]. These factors exert multi-level regulatory effects during the healing process: VEGF promotes neovascularization and improves blood supply at the interface, particularly relevant given that insufficient vascularity is a key factor limiting tendon healing—while TGF-β and bFGF induce mesenchymal stem cell chondrogenic differentiation and fibrocartilage regeneration[22]. The use of PRP in gel form, as opposed to liquid PRP, enables sustained local retention and prolonged bioactivity of growth factors, which may account for the favourable outcomes observed in the PRP group.

The LIPUS group also showed significant improvements over the control group across all measured parameters, further validating the efficacy of LIPUS as a non-invasive physical therapy for promoting tendon–bone healing. Recent studies have begun to elucidate the molecular mechanisms underlying this effect. Yang et al.[23] reported that LIPUS promotes the polarization of local macrophages towards the M2 anti-inflammatory phenotype, creating an immunomodulatory milieu conducive to tissue regeneration. M2 macrophages secrete anti-inflammatory and pro-repair factors that further enhance osteogenic and chondrogenic differentiation of bone marrow-derived mesenchymal stem cells. Moreover, the mechanical stimulation provided by LIPUS can directly activate intracellular mechanotransduction pathways, promoting proliferation and matrix synthesis in tenocytes and osteoblasts[24-26]. Our histological and biomechanical findings provide direct evidence for the therapeutic efficacy of LIPUS, corroborating the proposed mechanisms.

Our results build on, rather than duplicate, earlier work on combining PRP with

mechanical stimulation. Peng et al. demonstrated in mice that PRP plus active treadmill exercise improved early rotator-cuff healing[14]. The present strategy differs in the type and delivery of the mechanical stimulus and in the PRP formulation. First, LIPUS is a non-invasive, locally applied acoustic mechanical stimulus (30 mW/cm², 1.5 MHz, 20% duty cycle) that does not require active movement and can be delivered from the first postoperative week at a precisely controlled dose, making it suitable for the early, relatively immobilized rehabilitation window when active exercise is impractical or risky, and readily translatable to a bedside or wearable setting. Second, we used a thrombin/calcium-activated PRP gel that forms a fibrin scaffold for localized, sustained growth-factor release, addressing the rapid dispersion of liquid PRP. These features distinguish the present regimen from exercise-based combination protocols and extend the multimodal options for early postoperative rehabilitation.

The most notable finding of this study is that the combined group significantly outperformed both the LIPUS and PRP groups at both postoperative time points, indicating a clear additive benefit of the combined regimen over either modality alone. From a temporal perspective, growth factors released from the PRP gel in the early postoperative period provide a sustained supply of bioactive molecules during the inflammatory and reparative phases, whereas LIPUS stimulation persists throughout the healing process, continuously modulating cellular behaviour and the local microenvironment, thus forming a sequential and additive effect. Furthermore, in terms of target mechanisms, PRP primarily supplies a broad repertoire of growth factors and active proteins, while LIPUS enhances cellular responsiveness to these factors through mechanosignalling, suggesting possible convergence at shared mechanosignalling pathways. In addition, PRP gel serves as a three-dimensional scaffold supporting cell migration and tissue ingrowth, while intermittent LIPUS stimulation facilitates the ordered alignment and mechanical remodelling of newly formed collagen fibres, complementary actions in tissue architectural restoration. Notably, the superiority of the combined group remained significant at 8 weeks, suggesting that the superiority of the combined regimen is not merely a short-term

benefit, but rather that early higher-quality healing establishes a better foundation for subsequent tissue remodelling and mechanical strengthening. This finding holds important clinical implications. Retears after rotator cuff repair predominantly occur between 6 and 26 weeks post-surgery, the early phase of tendon‐bone healing. If the quality of interface healing can be substantially improved during this critical window through combined intervention, this early improvement may motivate future long-term studies of whether such enhancement translates to lower retear rates. First, the rat rotator cuff injury model differs from the human condition in terms of anatomical structure, mechanical environment and healing dynamics, and caution is warranted when extrapolating our findings to clinical practice. The supraspinatus tendon in rats is relatively small, and its healing kinetics may not fully reflect those of larger human rotator cuff tendons. Second, we only evaluated early healing up to 8 weeks post-surgery and did not assess long-term outcomes or retear risk. Furthermore, the PRP preparation protocol, platelet concentration, activation method and optimal LIPUS parameters require further optimization and standardization. Future studies using larger animal models are needed to validate the combined therapeutic effect and to evaluate its impact on long-term interface maturation and mechanical properties.

In conclusion, the combined application of PRP gel and LIPUS further promotes early tendon‐bone interface healing after acute rotator cuff repair, with significant superiority over either treatment alone across histological, radiological and biomechanical dimensions. PRP gel is relatively easy to prepare, autologous and non-immunogenic, while LIPUS is non-invasive and safe, both modalities are practically feasible in clinical settings. This combined strategy holds promise as an effective adjunct to postoperative rehabilitation protocols and has considerable translational potential. Prospective randomized controlled trials in patients with rotator cuff tears are warranted to further validate its clinical efficacy and safety.

**Author contributions**

Conceptualization: Junhong Chen and Xu Peng. Data curation: Qingshan Li. Funding acquisition: Xu Peng. Methodology: Xu Peng, Qiuling Shi and Junhong Chen. Project administration: Junhong Chen and Xu Peng. Software: Libin Li and Xin Guo. Writing

– original draft: Junhong Chen. Writing – review & editing: Xu Peng and Qiuling Shi. All authors have read and agreed to the published version of the manuscript.

**Funding**

This work was Supported by Foundation of State KeyLaboratory of Ultrasound in Medicine and Engineering(Grant No. 2023KFKT024)

**Data availability**

The datasets used and/or analysed during the current study are available from the corresponding author on reasonable request

**Declarations**

**Ethics approval and consent to participate**

This study has been approved by the Ethics Committee of Suining Central Hospital (Approval No.: SYDWLL21-2411-6)

**Competing interests**

The authors declare no competing interests

**Author details**

[1]Lower Extremity Trauma and Orthopaedics, Suining Central Hospital, Suining, 629000, China

[2]State Key Laboratory of Ultrasound in Medicineand Engineering, Chongqing Medical University, Chongqing, 400016, China

[3]Department of Orthopaedics, Suining Central Hospital, Suining, 629000, China

[1] Zong LZ, Duan MM, Yuan WW, et al. Efficacy of shoulder arthroscopic surgery for the treatment of rotator cuff injury: A protocol of systematic review and meta-analysis[J]. Medicine, 2020, 99(26):e20591.

[2] Anupama P, Varadraj N V, Enid S, et al. Growth factor delivery strategies for rotator cuff repair and regeneration[J]. Int J Pharm, 2018, 544(2):358-371.

[3] Benjamin M, Mcgonagle D. Entheses: tendon and ligament attachment sites[J]. Scand J Med Sci Sports, 2010, 19(4):520-527.

[4] Atesok K, Fu FH, Wolf MR, et al. Augmentation of Tendon-to-Bone Healing[J]. J Bone Joint Surg Am, 2014, 96(6):513-521.

[5] Mats C R, Hanna C BH, Theresa H, et al. Surgery and physiotherapy were both successful in the treatment of small, acute, traumatic rotator cuff tears: a prospective randomized trial[J]. Shoulder Elbow Surg, 2020, 29(3):459-470.

[6] Yu WX, Xu P, Huang GL, et al. clinical therapy of hyaluronic acid combined with

platelet-rich plasma for the treatment of knee osteoarthritis[J]. Exp Ther Med, 2018, 16:2119–2125.

[7] Chen X, Jones IA, Park C, et al. The Efficacy of Platelet-Rich Plasma on Tendon and Ligament Healing: A Systematic Review and Meta-analysis With Bias Assessment[J]. Am J Sports Med, 2018, 46(8):2020-2032.

[8] Hurley ET, Lim Fat D, Moran CJ, et al. The Efficacy of Platelet-Rich Plasma and Platelet-Rich Fibrin in Arthroscopic Rotator Cuff Repair: A Meta-analysis of Randomized Controlled Trials[J]. Am J Sports Med, 2019, 47(3):753–761.

[9] Byron C, Panagiotis G, Pericles P, et al. Molecular and Biologic Effects of Platelet-Rich Plasma (PRP) in Ligament and Tendon Healing and Regeneration: A Systematic Review[J]. Int J Mol Sci, 2023, 24(3):2744.

[10] Cai YZ, Zhang C, Lin XJ. Efficacy of platelet-rich plasma in arthroscopic repair of full-thickness rotator cuff tears: a meta-analysis[J]. J Shoulder Elbow Surg, 2015, 24(12):1852-18599.

[11] Jo CH, Roh YH, Kim JE, et al. Optimizing platelet-rich plasma gel formation by varying time and gravitational forces during centrifugation[J]. J Oral Implantol, 2013, 39(5):525-532.

[12] Wang JW, Lai B, Nanayakkara G, et al. Experimental data-mining analyses reveal new roles of low-intensity ultrasound in differentiating cell death regulatome in cancer and non-cancer cells via potential modulation of chromatin long-range interactions[J]. Front Oncol, 2019, 9(0):600.

[13] Lu HB, Chen C, Qu J, et al. Initiation Timing of Low-Intensity Pulsed Ultrasound Stimulation for Tendon-Bone Healing in a Rabbit Model[J]. Am J Sports Med, 2016, 44(10):2706-2715.

[14] Peng YD, Li XM, Wu WX, et al. Effect of Mechanical Stimulation Combined With Platelet-Rich Plasma on Healing of the Rotator Cuff in a Murine Model[J]. Am J Sports Med, 2022, 50(5):1358-1368.

[15] Landesberg R, Roy M, Glickman RS. Quantification of growth factor levels using a simplified method of platelet-rich plasma gel preparation[J]. J Oral Maxillofac Surg, 2020, 58(3):297-399.

[16] Lebaschi AH, Deng XH, Camp CL, et al. Biomechanical, histologic, and molecular evaluation of tendon healing in a new murine model of rotator cuff repair[J]. Arthroscopy, 2018, 34(4):1173-1183.

[17] Lai WC, Iglesias BC, Mark BJ, et al. Low-intensity pulsed ultrasound augments tendon, ligament, and bone-soft tissue healing in preclinical animal models: A systematic review[J]. Arthroscopy, 2021, 37(7):1-15.

[18] Naseri F, Dadgoo M, Pourahmadi M, et al. Dry needling as an adjunct treatment to multimodal rehabilitation protocol following rotator cuff repair surgery: a preliminary, randomized sham-controlled trial[J]. Chiropr Man Ther, 32(1):39.

[19] Kurtaliaj I, Hoppe ED, Huang Y, et al. Python tooth-inspired fixation device for enhanced rotator cuff repair[J]. Sci Adv, 2024, 10(26):eadl5270.

[20] Lu HH, Thomopoulos S. Functional Attachment of Soft Tissues to Bone: Development, Healing, and Tissue Engineering[J]. Annu Rev Biomed Eng, 2013, 15(1):201-226.

[21] Han F, Xia ZG, Chen QY, et al. Influence and mechanism of platelet-rich plasma gel on layered skin flap transplantation in rats and its mechanism[J]. Anhui Medical Journal, 2024, 45(10):1215-1221.

[22] Liu SR, Xu ZH, Zhao YM, et al. Research progress on bone regeneration through the combined application of platelet-rich plasma and mesenchymal stem cells[J]. Medical Journal of the Chinese People's Armed Police Force, 2025, 36(2):177-180.

[23] Yang G, Xu ZH, Li SC, et al. The mechanism of low-intensity pulsed ultrasound accelerating tendon bone interface healing[J]. Chinese Journal of Experimental Surgery, 2022, 39(11):2077-2080.

[24] Suzuki A, Takayama T, Suzuki N, et al. Daily low-intensity pulsed ultrasound-mediated osteogenic differentiation in rat osteoblasts[J]. Acta Biochim Biophys Sin, 2009, 41(2):108-115.

[25] Hu JZ, Qu J, Xu DQ, et al. Combined application of low-intensity pulsed ultrasound and functional electrical stimulation accelerates bone-tendon junction healing in a rabbit model[J]. J Orthop Res, 2014, 32(2):204-209.

[26] Vedran L, Michael L, Jerome G, et al. The effects of low-intensity pulsed ultrasound on tendon-bone healing in a transosseous-equivalent sheep rotator cuff model[J]. Knee Surg Sports Traumatol Arthrosc, 2012, 21(2):466-475.